Reaction of Thiols with Phenylglyoxal To Give Thiolesters of Mandelic Acid. 2.[1] Intramolecular General-Base Catalysis and Change in Rate-Determining Step

Tadashi Okuyama,* Shinji Komoguchi, and Takayuki Fueno

Contribution from the Faculty of Engineering Science, Osaka University, Toyonaka, Osaka 560, Japan. *Received August 7, 1981*

Abstract: Reactions of phenylglyoxal (**1**) with *N*-(2-mercaptoethyl)morpholine (**2a**) and -piperidine (**2b**) to give the thiolesters (**4**) of mandelic acid have been kinetically investigated at 30 °C. The reaction proceeds through the initial formation of a hemithioacetal (**3**) (rapid equilibrium with the equilibrium constant K_h = 400–1500 M^{-1}) and its rearrangement via the intramolecular general-base-catalyzed proton transfers to form **4**. The pH–rate profile and primary kinetic isotope effects showed that the deprotonation to form an enediol intermediate (**5**) is rate determining in the reaction with **2a**. In the case of **2b**, a change in the rate-determining step was observed. At pH <8 the deprotonation is rate determining, but at higher pH(D) the isotope exchange between the α hydrogen of **3** and the solvent deuterium (in D_2O) was found by both NMR and kinetic analysis; the reprotonation of **5** to form **4** becomes rate determining. Any significant metal ion catalysis was not detected with Zn^{2+}, Mg^{2+}, and Ca^{2+} in aqueous solutions even at low ionic strength.

Franzen[2,3] earlier found that 2-dialkylaminoethanethiols are efficient catalysts for the Cannizzaro-type rearrangement of phenyl- and methylglyoxals to the α-hydroxy acids. These observations have been widely known as a classic example of enzyme-model reactions, which mimicks the glyoxalase–glutathione system.[4] No mechanistic investigations have been undertaken on this model reaction until recently. A mechanism presented by Franzen,[2,3] which involves a 1,2-hydride transfer facilitated by an internal base (eq 1) and was often cited in popular text-

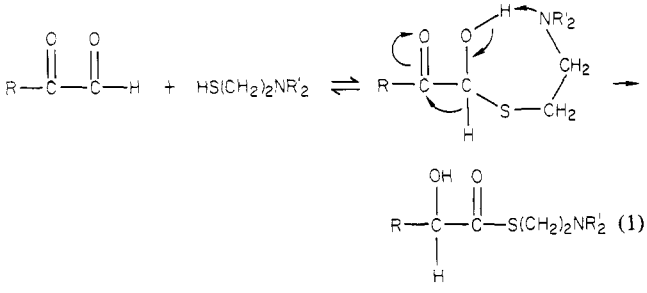

books,[5] has recently been disregarded by the isotope incorporation experiments.[6]

A mechanism involving proton transfer through an enediol intermediate has been proposed on the basis of the observation that a solvent hydrogen was incorporated in the product[6] (eq 2).

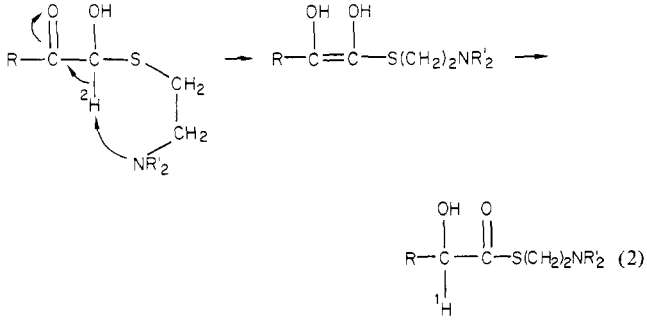

This latter mechanism was supported by the flavin-trapping of the enediol intermediate.[7] The enzymatic reaction by glyoxalase I was also concluded to proceed through a similar mechanism of fast-shielded enediol proton transfers.[6]

Our previous paper[1] showed that simple thiols catalyze the Cannizzaro-type rearrangement of phenylglyoxal through a similar mechanism involving the intermediate formation of a hemithioacetal and an enediol. The rate-determining step was found to be a general-base-catalyzed deprotonation to form the enediol. The present paper deals with the intramolecular general-base catalysis in the reaction of phenylglyoxal (**1**) with thiols carrying

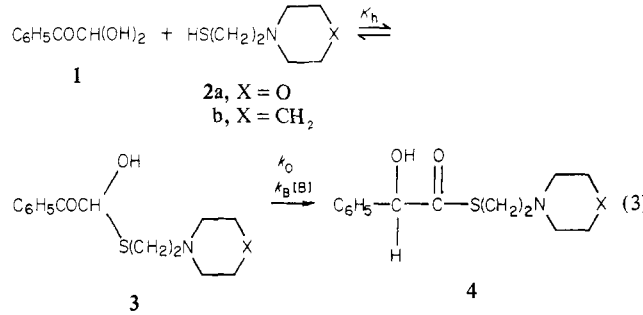

morpholino (**2a**) and piperidino groups (**2b**). The deprotonation of the α hydrogen of the hemithioacetal **3** by an internal base (amine) to form an enediol intermediate was found to usually be a rate-determining step. However, at higher pH (>8) the protonation of the enediol to give an α-hydroxy thiolester **4** became rate determining in the reaction of **1** with **2b**.

Experimental Section

Materials. Phenylglyoxal (**1**) hydrate was prepared as described previously.[1] Phenylglyoxal-*1*-d_1 (**1**-*d*) was prepared in the same way as **1** from acetophenone-d_3, which was obtained by three successive isotope exchanges in 1 M NaOD in D_2O. The product was purified as a hydrate by recrystallization from water: white needles, mp 76–77 °C. The ^1H NMR spectrum in D_2O showed only multiplets due to the phenyl group. *N*-(2-Mercaptoethyl)morpholine (**2a**) and *N*-(2-mercaptoethyl)piperidine (**2b**) were prepared according to the method of Johnson.[8] **2a**: bp 109–110 °C (22 mm) [lit.[3] 102 °C (14 mm)]. **2b**: bp 81–82 °C (11 mm) [lit.[3] 84–87 °C (16 mm)]. All the other chemicals used were obtained as described previously.

Kinetic Measurements were carried out spectrophotometrically at 30 °C in the same way as before.[1] A Shimadzu UV-200 spectrophotometer

(1) Part I: Okuyama, T.; Kimura, K.; Fueno, T. *Bull. Chem. Soc. Jpn.*, in press.
(2) Frazen, V. *Chem. Ber.* **1955**, *88*, 1361–1367.
(3) Franzen, V. *Chem. Ber.* **1957**, *90*, 623–633.
(4) Franzen, V. *Chem. Ber.* **1956**, *89*, 1020–1023.
(5) E.g.: (a) Mahler, H. R.; Cordes, E. H. "Biological Chemistry", 2nd ed.; Harper & Row: New York, 1966; pp 392–393. (b) Jencks, W. P. "Catalysis in Chemistry and Enzymology"; McGraw-Hill: New York, 1969; p 158.
(6) (a) Hall, S. S.; Doweyko, A. M.; Jordan, F. *J. Am. Chem. Soc.* **1976**, *98*, 7460–7461. (b) Hall, S. S.; Doweyko, A. M.; Jordan, F. *Ibid.* **1978**, *100*, 5934–5939.
(7) (a) Shinkai, S.; Yamashita, T.; Kusano, Y.; Manabe, O. *Chem. Lett.* **1979**, 1323–1326. (b) Shinkai, S.; Yamashita, T.; Kusano, Y.; Manabe, O. *J. Am. Chem. Soc.* **1981**, *103*, 2070–2074.
(8) Johnson, D. L. U. S. Patent 3 260 718, 1966; *Chem. Abstr.* **1966**, *65*, 15174a.

0002-7863/82/1504-2582$01.25/0

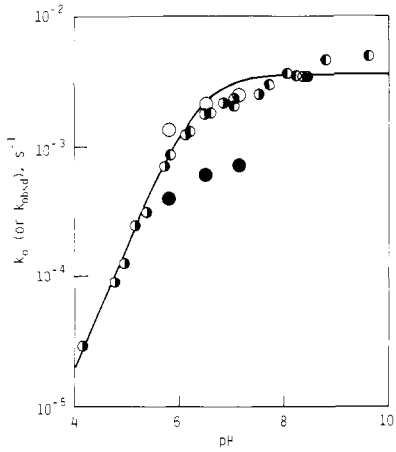

Figure 1. pH–rate profile for the reaction of **1** with **2a** at 30 °C. The k_0 values are calculated from k_{max} (◐) or k_0' (◑) obtained for the reactions in buffer solutions of μ = 0.475. Open and closed circles are k_{obsd} for **1** and **1**-*d* at [**2a**] = 0.043 M and μ = 0.075, respectively.

was used. Solutions of **2a** and **2b** in freshly boiled glass-distilled water were prepared under nitrogen immediately before use and contained 10^{-4} M EDTA except for the solutions containing Ca^{2+}, Mg^{2+}, or Zn^{2+}. Concentrations of thiols were assayed by the Ellman method.[9] For the pH determinations of thiol-containing solutions on a Hitachi-Horiba F-7 pH meter, special care was taken to avoid the deterioration of a silver–silver chloride electrode by permitting a short contact and soaking the electrode in a 0.1 M HCl solution after each measurement. The pH values may be accurate within to ±0.03.

The pD values of deuterium solutions were determined by adding 0.40 to the pH meter readings.[10]

NMR Analysis of the Reaction Mixtures. In a small reagent tube was placed 1 mL of 0.05 M DCl in 20% CD_3CN/D_2O (v/v); dry nitrogen was bubbled in for 5 min. Into this solution was dissolved 40 mg (0.26 mmol) of **1** recrystallized from D_2O. To the resulted mixture, 45 μL (ca. 0.3 mmol) of **2b** was added with a microsyringe at room temperature (25 °C). The reaction mixture became turbid immediately and was shaken vigorously. An aliquot (0.3 mL) of the mixture was taken with a syringe at an appropriate reaction time and immediately quenched by mixing with 0.1 mL of 1 M DCl in an NMR sample tube. The ^1H NMR spectra were recorded on a JEOL Model JNM FX-100 spectrometer.

Results

The kinetic behavior of the reaction of phenylglyoxal (**1**) with amino thiols **2a** and **2b** is essentially the same as that observed with simple thiols.[1] On addition of the stock solution of **1** into a buffer solution containing **2**, the absorption in the 280-nm region increased very rapidly and then decreased slowly. The initial absorbance increase corresponds to the formation of a hemithioacetal **3** and the following decrease to its rearrangement to the α-hydroxy thiolester **4** (eq 3).

The rates of the rearrangement were determined by following the latter decrease in the UV absorption (280 or 285 nm). The observed rate constants k_{obsd} were dependent both on the thiol and buffer concentrations as observed previously with simple thiols.[1] In buffer solutions of a constant buffer ratio (pH) and concentration, k_{obsd} increases with increasing thiol concentrations but shows saturation with a maximum rate constant k_{max} (eq 4). The

$$k_{obsd} = k_{max}K_h[\mathbf{2}]/(1 + K_h[\mathbf{2}]) \quad (4)$$

constant K_h corresponds to the equilibrium constant for the formation of the hemithioacetal **3**. At constant thiol concentrations and pH, k_{obsd} usually increases linearly with total buffer concentrations $[B]_t$ as described in the equation

$$k_{obsd} = k_0' + k_{Bt}'[B]_t \quad (5)$$

Combining eq 4 and 5, k_{max} is expressed by

$$k_{max} = k_0 + k_{Bt}[B]_t \quad (6)$$

(9) Ellman, G. L. *Arch. Biochem. Biophys.* **1959**, *82*, 70–77.
(10) Bates, R. G. "Determination of pH"; Wiley: New York, 1973; pp 375–376.

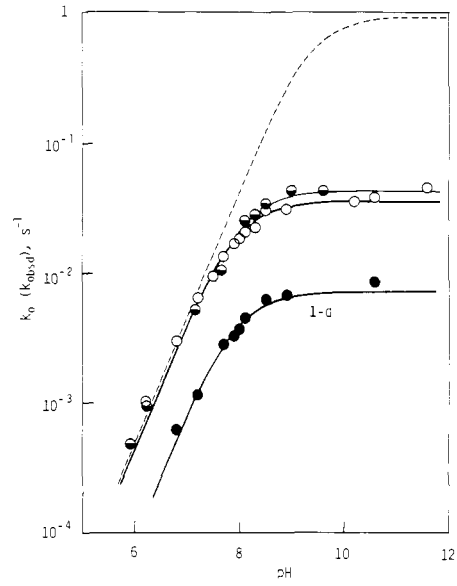

Figure 2. pH–rate profiles for the reaction of **1** and **1**-*d* with **2b** at 30 °C: ⊖, k_0 for **1** at μ = 0.475; ○, k_{obsd} for **1** at [**2b**] = 0.045 M and μ = 0.05–0.08; ●, k_{obsd} for **1**-*d* at [**2b**] = 0.045 M and μ = 0.05–0.08.

Kinetic parameters obtained in this way are summarized in Tables S1–S3 (supplementary material) for the reactions of **1** with **2a** and **2b**. The values of K_h change with pH (300–1600 M^{-1}) but are considered to be independent of buffer concentrations. The rate constants k_0 and k_{Bt} are calculated from k_0' and k_{Bt}' by multiplying them by the factor $(1 + K_h[\mathbf{2}])/K_h[\mathbf{2}]$. After k_{Bt} is found, the k_0 values are obtained from k_{max} according to eq 6. The buffer-independent rate constants k_0 are logarithmically plotted against pH for **2a** and **2b** in Figures 1 and 2, respectively, with half-filled circles for the reactions in aqueous solutions containing 5 vol % acetonitrile at ionic strength of 0.475 adjusted with KCl.

In the presence of high concentrations of thiols ($[\mathbf{2}] >> 1/K_h$), the k_{obsd} values are equal to k_{max}. At a moderate thiol concentration where $K_h[\mathbf{2}]/(1 + K_h[\mathbf{2}])$ is satisfactorily close to unity and its effect as an external (bimolecular) base is still negligible, k_{obsd} is nearly equal to k_0. Without added buffers, pH can be maintained over the considerable range of pH by the buffer function of the thiol itself. The observed rate constants k_{obsd} obtained under such conditions at low ionic strength (<0.1) are plotted with open circles for **2a** ([**2a**] = 0.043 M) and **2b** ([**2b**] = 0.045 M) in Figures 1 and 2, respectively; the data are available in Tables S4 and S5. Under these conditions, $K_h[\mathbf{2}]/(1 + K_h[\mathbf{2}]) > 0.95$. All the points fall close to the line of k_0 obtained in buffer solutions of ionic strength of 0.475. Effects of ionic strength were found to be in fact very small for the present reaction (the data are included in Tables S4 and S5). Effects of dipositive metal ions, Ca^{2+}, Mg^{2+}, and Zn^{2+}, were found to be negligibly small for the reaction of **1** with **2b** even at a low ionic strength of 0.08, the greatest being a 5% rate increase with 0.01 M $MgCl_2$ (the data in Table S6).

Primary kinetic isotope effects were examined with deuterated substrate **1**-*d* without using external buffers. The values of log k_{obsd} are plotted against pH with closed circles in Figures 1 and 2; the data are given in Tables S4 and S5. Pseudo-first-order plots for the reaction of **1**-*d* in the solution of **2b** at higher pH (>8.5) showed small downward curvature (acceleration). The rate constants k_{obsd} were obtained from the initial linear parts within a half-time. The deuterium substrate **1**-*d* is less reactive than **1** by factors of ~3.5 and 5 for the reactions with **2a** and **2b**, respectively.

Reactions were also carried out in deuterium media. Without using external buffers, the reaction solutions for kinetic measurements contained a constant concentration of **2b** (0.045 M), and the pD was adjusted by the addition of DCl or NaOD. The reactions of the deuterated substrate **1**-*d* followed perfect pseu-

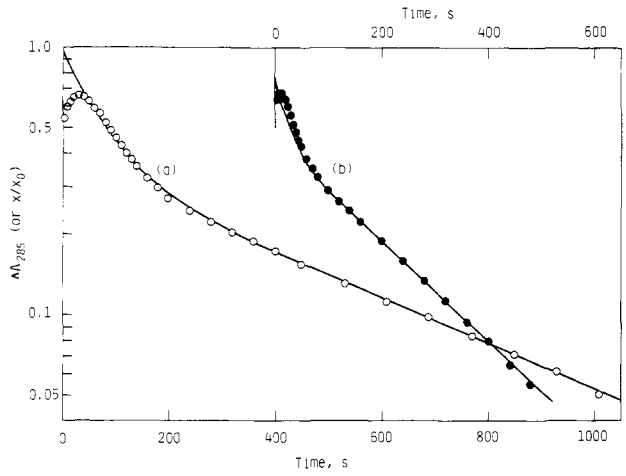

Figure 3. Changes in absorbance at 285 nm as a function of time for the reaction of **1** with **2b** in D_2O at pD 8.15 (○) and 8.9 (●). Curves are theoretical ones based on eq 15: (a) $k_1/k_1' = 5$ and $k_2'/k_{-1}' = 2$; (b) $k_1/k_1' = 5$ and $k_2'/k_{-1}' = 1$. Time scales are chosen arbitrarily to fit the ultimate linear plots.

do-first-order kinetics for all the runs. By contrast, pseudo-first-order plots for the reactions of **1** curved strongly upward at pD 8.15 and 8.9 as shown in Figure 3, although the plot was satisfactorily linear at a lower pD of 7.4. The initial increase in absorption must be due to the hemithioacetal formation. The ultimate slopes (after 80% reaction) of the curved plots agree well with the slopes for **1**-*d*. The observed rate constants are summarized in Table S7.

The progress of the reaction of **1** with **2b** in D_2O was followed by ^1H NMR spectroscopy. The reaction was carried out in 20% CD_3CN/D_2O (v/v) at a buffer ratio $\mathbf{2bD^+/2b} \simeq 1/5$ under a nitrogen atmosphere. Into the solution containing appropriate amounts of DCl (0.05 M) and **1** (0.26 M), **2b** (0.3 M) was added at room temperature. The reaction mixture was shaken vigorously; it became turbid probably owing to the formation of the hemithioacetal **3b**. An aliquot of the turbid solution was taken and immediately acidified by the addition of 1 M DCl to quench the reaction. The resulted transparent sample solution was subjected to the NMR analysis. Spectra a and b of Figure 4 show mixtures of reaction times of 1 and 2 min, respectively. The resolution of spectrum b is rather poor because of a slight turbidity of the sample. Signals in the phenyl resonance region may be divided into three groups. The multiplet (doublet of triplet) at 7.9–8.2 ppm (centered at 8.05 ppm) must be due to the ortho hydrogens of the hemithioacetal **3b**. The multiplet appearing between 7.2 and 7.7 ppm has an intensity of 1.5 times that of the multiplet centered at 8.05 ppm and is ascribed to the other three hydrogens of the phenyl group of **3b**. The remaining sharp signal at 7.2 ppm increases in intensity as the reaction proceeds and conforms to the phenyl resonance of the product, thiomandelate ester **4b**. The singlet at 6.1 ppm is due to the α hydrogen of **3b**. The integrated intensity of this singlet should be originally half that of the multiplet at 8.05 ppm as found for the closely resembled spectrum of the hydrate of **1**. The intensity ratios of these two signals are 0.44 and 0.39 for spectra a and b, respectively. This indicates that the α hydrogen of **3b** is partially lost during the reaction. The extent of the rearrangement can be estimated from the relative intensity of the signal at 7.2 ppm to the total phenyl intensity, about 15 and 30% reactions for spectra a and b, respectively. Furthermore, the signal due to the α hydrogen of the product thiolester **4b**, which was to appear at about 5.0 ppm, was not detected.

Discussion

Dissociation Constants of the Amino Thiols. Before we analyze the kinetic results, it is useful to know the microscopic dissociation constants of the amino thiols **2a** and **2b**. We have determined spectrophotometrically the dissociation constants of **2a** and **2b** in 5% aqueous acetonitrile at an ionic strength of 0.475 (KCl) and

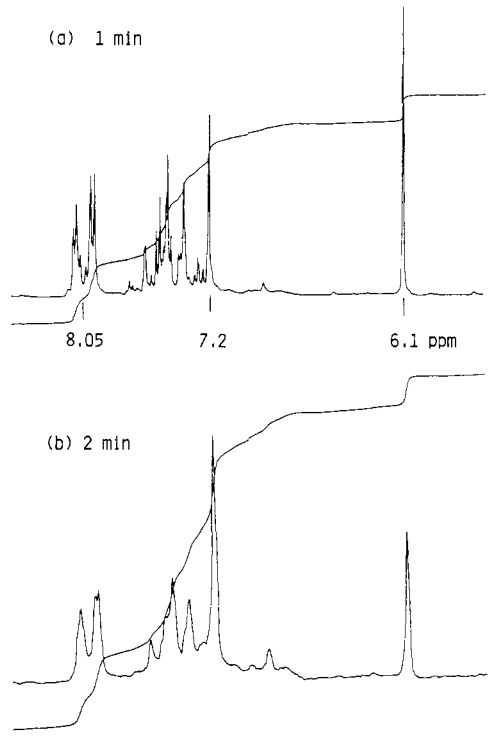

Figure 4. ^1H NMR spectra of the quenched mixtures of the reaction of **1** with **2b** in 20% CD_3CN/D_2O at the reaction times of 1 min (a) and 2 min (b).

30 °C: $pK_a = 9.57$ (**2a**) and 7.90 (**2b**).[11] These values are due to the ionization of the thiol group. From the pH values of half-neutralized buffer solutions, the other pK_a values were found to be about 6.8 and 11.5 for **2a** and **2b**, respectively. From these values microscopic pK_a values for the ionizations of **2a** and **2b** are estimated as shown in eq 7 and 8, respectively.

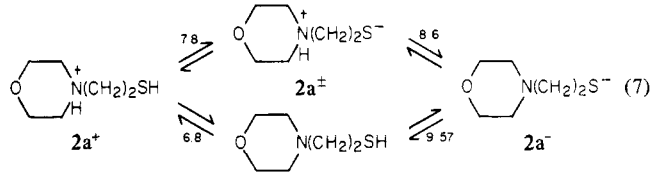

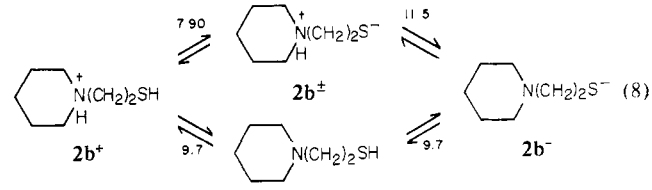

2b

The values for the processes $\mathbf{2a^+ \rightleftharpoons 2a^{\pm}}$ and $\mathbf{2b \rightleftharpoons 2b^-}$ are assumed to be 0.1 pK unit different from the corresponding values for $\mathbf{2b^+}$ and **2a**, respectively. All the values assigned in eq 7 and 8 are mutually consistent and reasonable as compared with the pK_a's of morpholine (8.4) and piperidine (11.2).

Reaction of 1 with 2a. The reaction of phenylglyoxal (**1**) with amino thiols **2** proceeds essentially in the same way as that with simple thiols.[1] We first take a close look at the reaction of **1** with the morpholino thiol **2a**. The K_h values change remarkably with pH of the reaction media (500–1600 M^{-1}). It was previously found that the K_h values change with pH as the thiol ionizes.[1] The present observations may be rationalized, in the same way, by the

(11) Determined by the change in absorbance at 235 nm. Franzen[3] reported pK_a values in 50% aqueous methanol at 18 °C to be 6.65 and 9.80 for **2a** and 7.95 and 11.05 for **2b**.

Table I. Summary of the Kinetic Parameters for the Reaction of **1** with the Amino Thiols **2**

	2a	2b
K_h, M^{-1}	500 (**2a**$^+$) 1500 (**2a**)	400 (**2b**$^+$)
k_{Bt}/k_0,[a] M^{-1}	2.36	1.0
k_1K_3, M s^{-1}	1.8×10^{-9}	4.4×10^{-10}
pK_3	6.3	(9.2)[b]
k_1, s^{-1}	3.6×10^{-3}	(0.7)[b]
effective concn,[c] M	30	90

[a] Values obtained in a Dabco buffer of pH 8.5. [b] For an estimation, see text. [c] Estimated by comparing k_1 with bimolecular catalytic constants k_B for *N*-methylmorpholine (4.5×10^{-4} M^{-1} s^{-1}) and *N*-methylpiperidine (2.14×10^{-2} M^{-1} s^{-1}) in the 2-mercaptoethanol reaction.[1] The pK_a corrections for the base were made by the Brønsted $\beta = 0.5$.

dissociation of **2a** (eq 7) and the three equilibria for the hemithioacetal formations (eq 9–11). From the equilibrium cycle the

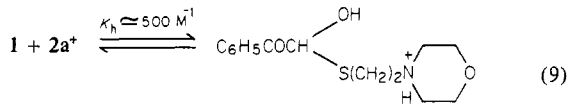

3a$^+$ (9)

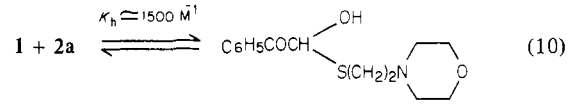

3a (10)

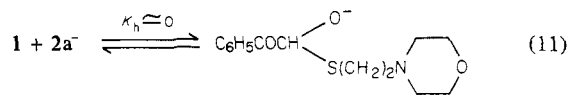

3a$^-$ (11)

pK_a value of the protonated hemithioacetal **3a**$^+$ (⇌**3a** + H^+) can be calculated to be 6.3.

The pH–rate profile of Figure 1 indicates that k_0 is inversely proportional to $[H^+]$ at lower pH and becomes independent of pH as pH increases, conforming to eq 12 with the parameters given

$$k_0 = k_1K_3/(K_3 + [H^+]) \quad (12)$$

in Table I. A reasonable mechanism for the kinetic results may involve a rate-determining deprotonation by the internal base within a neutral hemithioacetal **3a** to form an enediol **5a**, as

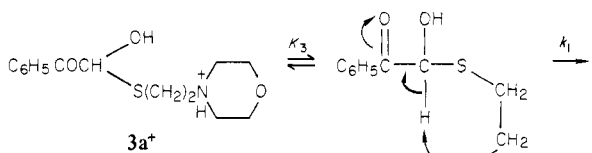

3a$^+$ **3a**

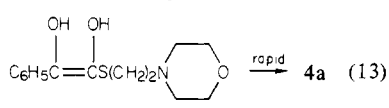

4a (13)

5a

suggested previously.[6,7] The water-catalyzed reaction of **3a**$^+$ has little contribution to the observed rates. The value K_3 corresponds to the dissociation constant of **3a**$^+$ in perfect agreement with the value obtained thermodynamically.

Apparent effects of external buffers are small in accord with the mechanism involving an internal base catalysis. For example, the ratio k_{Bt}/k_0 in a Dabco buffer of pH 8.5 is 2.36 M^{-1} for the **2a** reaction as compared with the value 31.4 M^{-1} for the reaction of 2-mercaptoethanol.[1] The primary kinetic isotope effect found

Table II. Kinetic Isotope Effects for the Reaction **1** with **2b**[a]

pH	primary KIE[b] k_H/k_D
6.8–8.0	5.03 ± 0.09
85.	4.68
8.9	4.43
10.6	4.38
pH (pD)	**solvent KIE[c] $k_{obsd}^{H_2O}/k_{obsd}^{D_2O}$**
6.9 (7.4)	1.13
7.6 (8.14)	1.21
8.4 (8.9)	1.36

[a] Measured without added buffers at 30 °C, [**2b**] = 0.045 M, $\mu <$ 0.1. [b] Relative rates of **1**/**1**-*d*. [c] Values for **1**-*d*.

with a deuterated substrate **1**-*d*, $k_H/k_D = 3.5$, and the negligible salt effects observed are also compatible with the mechanism of eq 13. A comparison of k_1 with a bimolecular general-base-catalytic constant for the 2-mercaptoethanol reaction[1] gives the effective concentration of the internal base to be about 30 M (Table I).

Reaction of 1 with 2b. The K_h values observed in the pH range 6–8 for the reaction of **1** with the piperidino thiol **2b** (~400 M^{-1}) seem to be rationalized by the fact that only the cationic thiol **2b**$^+$ has an appreciable contribution to the formation of the hemithioacetal. Apparent buffer effects on the rate of the rearrangement are significantly smaller than those for **2a** as seen in Table I. The intramolecular catalysis by the piperidino group may be stronger than the morpholino group.

The pH–rate profile of Figure 2 closely resembles that for **2a** in Figure 1. Analysis of the profile according to eq 12 gives apparent values of $k_1 = (3.5–4.4) \times 10^{-2}$ s^{-1} and $pK_3 = 7.9–8.0$. These values do not seem to be reasonable for a mechanism similar to that given for **2a** (eq 13). The value pK_3 is too small as compared with pK_a for the piperidinium group of **2b**$^+$ (9.7). Moreover, the k_1 value is also too small as compared with a bimolecular rate constant for *N*-methylpiperidine-catalyzed rearrangement of the hemithioacetal of 2-mercaptoethanol ($k_B = 2.14 \times 10^{-2}$ M^{-1} s^{-1}).[1]

The primary kinetic isotope effect examined with the deuterated substrate **1**-*d* in aqueous solutions is $k_H/k_D = 5.0$ below pH 8.0 and seems to decrease somewhat at higher pH as summarized in Table II. These values are greater than those found for **2a** and those obtained previously in general-base- and enzyme-catalyzed reactions: 2.3 for general base catalysis[6b] and 2.1–4.8 for enzyme catalysis.[12–14] In any case, the deprotonation step must be predominantly rate determining although the reprotonation of the enediol intermediate seems to become partially rate determining at higher pH.

The kinetic behavior of the reaction of **1** with **2b** in deuterium media is distinctly different from that observed in H_2O and that expected for the mechanism of rate-determining deprotonation to form the enediol intermediate. Pseudo-first-order plots markedly curve upward with an ultimate slope equal to the slope for **1**-*d* at higher pD (Figure 3). This strongly suggests that the isotope exchange occurs during the reaction. That is, the deprotonation to form the enediol is no more solely rate determining. In fact, ^1H NMR analysis of the reaction mixture showed loss of the α hydrogen of **3b** during the reaction in a deuterium medium of pD >8. At conversions of 15 and 30%, 12 and 22% of the α hydrogen was exchanged by the solvent deuterium, respectively.

In deuterium media, the rearrangement of the hemithioacetal **3b** may proceed according to Scheme I. By using the steady-state approximation, the kinetic equations shown in (14) and (15) can

$$x_1/x_0 = e^{-k_1t} \quad (14)$$

be derived where x = [**3b**] + [**3b**-*d*], x_1 = [**3b**], and the rate

(12) Vander Jagt, D. L.; Han, L.-P. B. *Biochemistry* **1973**, *12*, 5161–5167.
(13) Han, L.-P. B.; Davison, L. M.; Vander Jagt, D. L. *Biochim. Biophys. Acta* **1976**, *445*, 486–499.
(14) Han, L.-P. B.; Schimandle, C. M.; Davison, L. M.; Vander Jagt, D. L. *Biochemistry* **1977**, *16*, 5478–5484.

$$\frac{x}{x_0} = \frac{k_1k_2' - k_1'k_2'}{k_1k_{-1}' + k_1k_2' - k_1'k_2'}e^{-k_1t} + \frac{k_1k_{-1}'}{k_1k_{-1}' + k_1k_2' - k_1'k_2'}e^{-[k_1'k_2'/(k_{-1}'+k_2')]t} \quad (15)$$

constants are given in Scheme I. The initial concentration x_0 is solely due to **3b**, i.e., $x_0 = [\mathbf{3b}]_0$. The primary kinetic isotope effect on the deprotonation was found to be 5: $k_1/k_1' = 5$. A trial calculation with $k_2'/k_{-1}' = 2$ predicts that at the conversions of 15 and 30% the extents of deuterium incorporation are respectively 12 and 21%, in good agreement with the NMR observations. The calculated curve with these parameters is superimposed on the first-order plots of Figure 3 for the reaction of **1** with **2b** at pD 8.15. In the same way, the theoretical curve with $k_2'/k_{-1}' = 1$ is superimposed on the plots for the reaction at pD 8.9 in Figure 3. More precise simulations of the plots by the theoretical curves were difficult for us because of the large influence of the hemithioacetal formation on the kinetic analysis of the initial part of the reaction. However, the above illustrations show qualitatively that the value of k_2'/k_{-1}' becomes smaller as pD increases. That is, the rate of protonation (k_2) of the enediol **5b** to form the product **4b** becomes more influential on the observed rate as the pH increases.

A similar reaction scheme for the reaction of **1**-*d* in H_2O predicts that the first-order plots should curve slightly downward owing to the H–D exchange as the reaction proceeds. A kinetic equation similar to (15) with $k_2/k_{-1} = 2$ predicts satisfactorily linear plots within two half-times and a downward curvature toward the end of reaction in accord with the observations at higher pH. The slope of the initial apparently linear part gives a rate constant about 10% greater than k_1'. This reasonably accounts for the observed primary isotope effects which tend to decrease at higher pH (>8) as given in Table II.

Deuterium solvent isotope effects on the reaction of **1**-*d* are estimated as follows. First, solvent isotope effects on the dissociation constant K_3 for the internal ammonio groups of $\mathbf{3b}^+$ are evaluated by using the known fractionation factors.[15]

$$K_3^{H_2O}/K_3^{D_2O} = \phi_{NL}^{+}\phi_{OL}^{2}/\phi_{OL}^{+3} \approx 1.5^3 \quad (16)$$

The difference in the pK_3 values in D_2O and H_2O, $pK_3^{D_2O} - pK_3^{H_2O}$, would be 0.53. Since the reaction is considered to proceed predominantly through the intramolecular proton transfers, the rate constants $k_{obsd}^{D_2O}$ observed in D_2O should be compared with $k_{obsd}^{H_2O}$ observed in H_2O of pH lower than the pD by 0.53 unit where the extent of dissociation of the internal amino group is the same. The values of $k_{obsd}^{H_2O}/k_{obsd}^{D_2O}$ of 1.13–1.36 are thus obtained as given in Table II. The values close to unity and increasing with pH(D) are in accord with the mechanism that the deprotonation (k_1) is predominantly rate determining at lower pH and the protonation of the enediol **5b** to form the thiolester **4b** (k_2) increasingly contributes to the observed rate as pH increases.

A possible mechanistic change from the enediol proton transfer to the 1,2 hydride shift (an intramolecular Cannizzaro reaction) at higher pH can be excluded by the observed incorporation of a solvent deuterium into the product. The pH–rate profile of Figure 2 must be explained simply by the change in the rate-determining step of the enediol proton transfer. A detailed mechanism conforming to the observations is presented in Scheme II. Protonation of the enediol may take place mainly from the internal general acid either at the α (k_{-1}) or β position (k_2). The hydroxyl dissociation of the enediol (**5b** or $\mathbf{5b}^+$) may occur at pH as low as 8, as is the case for phenols, mainly at the β-OH group rather than at the α-OH (to give $\mathbf{5b}^{\pm}$ or $\mathbf{5b}^-$) as shown in Scheme II. Carbanion-stabilizing effects of an α-alkylthio group may well be greater than those of an α-phenyl group.[16] The enediolate ion $\mathbf{5b}^{\pm}$ protonates intramolecularly at the α position (k_{-1}^0), while

Scheme I

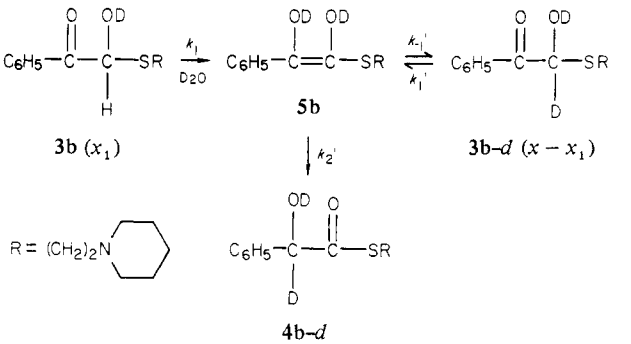

Scheme II

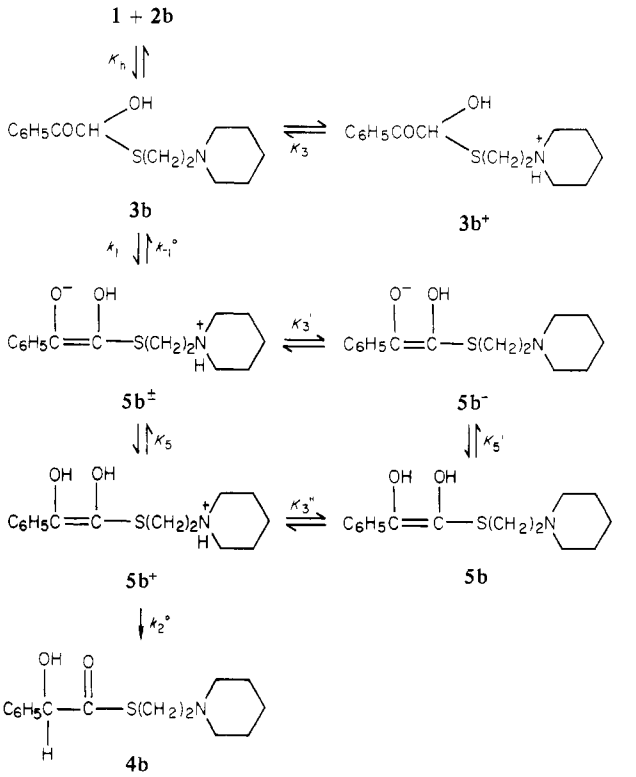

the protonation of $\mathbf{5b}^+$ may take place predominantly at the β position (k_2^0). Using kinetic parameters given in Scheme II, the buffer-independent rate constant k_0 can be described by eq 17.

$$k_0 = \frac{k_1k_2^0K_3[H^+]}{(k_{-1}^0K_5 + k_2^0[H^+])(K_3 + [H^+])} \quad (17)$$

Here we assume for simplicity that $K_3 = K_3' = K_3''$ and $K_5 = K_5'$. At pH << pK_3, eq 17 reduces to eq 18.

$$k_0 = \frac{k_1K_3}{k_{-1}^0K_5/k_2^0 + [H^+]} \quad (18)$$

The curve of Figure 2 gives values $k_{-1}^0K_5/k_2^0 = 10^{-8.0}$ and $k_1K_3 = 4.4 \times 10^{-10}$ M s^{-1} for the data at an ionic strength of 0.475. Plots for the lower ionic strength give $k_{-1}^0K_5/k_2^0 = 10^{-7.9}$ for both **1** and **1**-*d*, and $k_1K_3 = 4.4 \times 10^{-10}$ and 8.8×10^{-11} M s^{-1} for **1** and **1**-*d*, respectively. The pK_3 value for $\mathbf{3b}^+$ may be estimated to be 9.2 as compared with the amine pK_a of $\mathbf{2b}^+$ (9.7). The value $k_1 = 0.7$ s^{-1} is in turn obtained for **1**. The effective concentration of the internal base can now be evaluated to be ca. 90 M, threefold greater than that for the morpholino group. A hypothetical pH–rate curve according to the mechanism of a rate-determining deprotonation without a change in the rate-determining step is drawn by a dashed line in Figure 2.

According to the mechanism of Scheme II, a change in the rate-determining step occurs as **5b** dissociates. The higher the

(15) Schowen, R. L. *Prog. Phys. Org. Chem.* **1972**, *9*, 275–332.
(16) Bordwell, F. G.; Bares, J. E.; Bartmess, J. E.; Drucker, G. E.; Gerhold, J.; McCollum, G. J.; Van Der Puy, M.; Vanier, N. R.; Matthews, W. S. *J. Org. Chem.* **1977**, *42*, 326–332.

pH, the smaller the k_2/k_{-1} value, the k_2 step becoming rate determining. This tendency was found in the curvature of the pseudo-first-order plots for the reaction of **1** with **2b** in D_2O (Figure 3). In the reaction with simple thiols, a change in the rate-determining step does not seem to occur. This may be rationalized by the consideration that the intramolecular acceleration of the k_{-1}^0 process is greater than that of the k_2^0 process and thus k_{-1}^0 becomes comparable to k_2^0 in magnitude. Without this acceleration k_2^0 must be much greater than k_{-1}^0 for simple thiols; a change in the rate-determining step occurs, if it does, only at very high pH. At any rate, the overall behavior of the reaction seems to be explainable by Scheme II, but more precisely each of the four ionized states of **5b** would have a different partitioning ratio k_2/k_{-1}. A more complex rate equation would be derived to account for the observations quantitatively.

Metal Ion Catalysis and Implication to the Enzymatic Reaction. It has recently been found that glyoxalase I contains a tightly bound zinc ion which is essential for enzymatic activity.[17] On the other hand, we have found that the Cannizzaro reaction (hydroxide ion catalyzed rearrangement) of phenylglyoxal is markedly accelerated by calcium ion at low ionic strength, but the specific effects of calcium ion almost disappear as the ionic strength increases.[18] Therefore, we have examined the effects of dipositive metal ions on the present reaction at a low ionic strength (Table S6). However, none of zinc, magnesium, and calcium ions showed significant effects on the rate of the rearrangement. On addition of $ZnCl_2$, the pH of the buffer solution of **2b** greatly decreased, probably owing to complex formation (eq 19).[19]

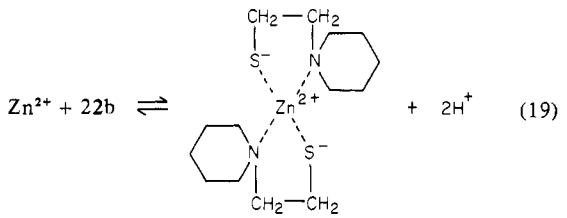

(19)

Hall and his co-workers found that magnesium ion accelerates the rearrangement of a hemithioacetal only slightly in aqueous solutions[6b] but remarkably in a nonaqueous solution.[20] Magnesium and some other dipositive metal ions reactivates inactive (metal-free) apo(glyoxalase I).[14,17,21] Furthermore, solvent incorporation studies of the glyoxalase reactions showed negligible[4,22] or low incorporation of solvent protons[6a] into the product, α-hydroxy acid. These observations strongly suggest that the active site of the enzyme is nonpolar enough to be subject to metal-ion catalysis and is highly protected to exclude a water molecule. Furthermore, an intramolecular catalysis of proton transfers to and from the enediol intermediate must play an important role in the enzyme reaction.

Comments on Previous Work. The existence of the enediol intermediate in the rearrangement of hemithioacetals of glyoxals was previously demonstrated by the solvent incorporation[6] and the flavin-trapping experiments.[7] Kinetic observations of the buffer-dependent rearrangement were briefly described by the former workers.[6b]

Shinkai et al.[7b] presented the results of flavin-trapping rate measurements. Although flavin-trapping rates are shown to be rapid enough to measure the rate of formation of the enediol, i.e., the rate of the rearrangement, their results are incompatible with ours in the important phase of the kinetics. The rates they obtained were first order in both thiol and glyoxal over thiol concentrations of $(1-6) \times 10^{-3}$ M. They justified this linearity by the incorrectly cited value of $K_h = 0.3\ M^{-1}$ for the hemithioacetal formation between methylglyoxal and glutathione; the literature gives the value 200 M^{-1} [23] in accord with the value obtained by other workers[24] and by us.[1] Furthermore, since we know that K_h varies greatly above pH 9, we suspect the significance of the pH–rate profiles and the Brønsted relation which they obtained without any corrections due to K_h. Their rate measurements were carried out by the *initial* velocity method. In the initial phase of this reaction, however, the formation of hemithioacetal strongly disturbs the kinetics of the rearrangement, as illustrated in Figure 3. We doubt that the flavin-trapping rate always measures the correct rate of the rearrangement. Moreover, they found that glutathione is a poor catalyst in borate buffers contrary to our observations that it is a very good catalyst in well-behaved buffers.[1,25] Their reasoning of catalytic inefficiency of glutathione due to Schiff base formation is hardly acceptable. The equilibrium would not favor the formation of such a Schiff base under the reaction conditions. Shinkai's demonstration of the enediol intermediate by the flavin-trapping is unique, but the kinetic results should be taken more carefully.

Registry No. 1, 1075-06-5; **1-*d***, 81027-63-6; **2a**, 4542-46-5; **2b**, 4706-22-3.

Supplementary Material Available: Tables S1–S3, kinetic data at ionic strength of 0.475; Tables S4 and S5, reactions without added buffers; Table S6, salt effects; Table S7, reactions in D_2O (7 pages). Ordering information is given on any current masthead page.

(17) Aronsson, A.-C.; Marmstål, E.; Mannervik, B. *Biochem. Biophys. Res. Commun.* **1978**, *81*, 1235–1240.
(18) Okuyama, T.; Kimura, K.; Fueno, T. *Bull. Chem. Soc. Jpn.*, in press.
(19) Coleman, J. E.; Vallee, B. L. *J. Biol. Chem.* **1961**, *236*, 2244–2249.
(20) Hall, S. S.; Poet, A. *Tetrahedron Lett.* **1970**, 2867–2868.
(21) Davis, K. A.; Williams, G. R. *Biochim. Biophys. Acta* **1966**, *113*, 393–395.
(22) Rose, I. A. *Biochim. Biophys. Acta* **1957**, *25*, 214–215.
(23) Kanchuger, M. S.; Byers, L. D. *J. Am. Chem. Soc.* **1979**, *101*, 3005–3010.
(24) Vander Jagt, D. L.; Han, L.-P. B.; Lehman, C. H. *Biochemistry* **1972**, *11*, 3735–3740.
(25) Borate forms unreactive complex with glyoxals[26] as noted. Glutathione is also inactivated easily by some reactions in borate buffers.
(26) Okuyama, T. unpublished results. See also for a similar complexation: Pasternak, R. *Helv. Chim. Acta* **1947**, *30*, 1984–1999.